Polymer 49 (2008) 2996–3006

Contents lists available at ScienceDirect

Polymer

journal homepage: www.elsevier.com/locate/polymer

Stimuli responsive associative polyampholytes based on ABCBA pentablock terpolymer architecture

C. Tsitsilianis [a,b,*], N. Stavrouli [a,b], V. Bocharova [c], S. Angelopoulos [a], A. Kiriy [c], I. Katsampas [a], M. Stamm [c]

[a] Department of Chemical Engineering, University of Patras, 26504 Patras, Greece
[b] Institute of Chemical Engineering and High Temperature Chemical Processes, ICE/HT-FORTH, P.O. Box 1414, 26504 Patras, Greece
[c] Leibniz-Institut für Polymerforschung Dresden, 01069 Dresden, Germany

ARTICLE INFO

Article history:
Received 3 March 2008
Received in revised form 21 April 2008
Accepted 26 April 2008
Available online 8 May 2008

Keywords:
Responsive reversible hydrogel
Rheological properties
Micelles

ABSTRACT

A poly(methyl methacrylate)–poly(acrylic acid)–poly(2-vinyl pyridine)–poly(acrylic acid)–poly(methyl methacrylate) (PMMA–PAA–P2VP–PAA–PMMA), ABCBA pentablock terpolymer was synthesized by "living" anionic polymerization and was studied in aqueous media at different pH conditions in the presence of MeOH. By tuning the pH and/or the solvent selectivity and dielectric constant of the medium, reversible hydrogels of different nature were formed. At low pH the hydrogel is based on a three dimensional network comprising PMMA hydrophobic cores (physical crosslinks) interconnected by complex bridging (elastically active) chains constituted of positively charged P2VP and non-ionic PAA segments. At high pH the hydrogel is transformed reversibly to a negatively charged network the bridging chains of which comprise ionized PAA segments interrupted by hydrophobic P2VP blocks, swellable on MeOH addition. Furthermore, we found conditions for the formation of flower-like micelles of different topologies and nature like core–shell–corona micelles with positively charged corona (pH < 2), multicompartment micelles comprising P2VP and PMMA hydrophobic domains (pH 8.3, low MeOH content), micelles constituted of a centrosymmetric compartmentalized core and PAA negatively charged corona (pH 8.3, 30%, 40% MeOH), and core–shell micelles of PMMA cores (pH 8.3, 50% MeOH).

1. Introduction

Associative water-soluble polymers are polymers that self-assemble through temporary junctions mainly of hydrophobic groups. Traditional associative polymers consist of neutral hydrophilic polymers containing hydrophobic associative groups. In this category, telechelic polymers (chains end-capped by hydrophobic groups) are often considered as a model of hydrophobic associative polymers [1–6]. Above a critical concentration, polymer chains self-associate in flower-like micelles constituted by a hydrophobic core, surrounded by a corona of hydrophilic polymer loops [7]. With increasing concentration, loop to bridge transitions occur leading to the interconnection of the flower-like micelles inducing a SOL–GEL transition which produces a sharp increase of the viscosity (thickeners). The unique rheological properties exhibited by the associative polymers, make them very useful materials as rheology modifiers in cosmetics and coatings, suspension stabilizers, drug carriers and injectable hydrogels in pharmaceutical formulations and other water-based applications.

Charged associative polymers (also named telechelic polyelectrolytes) have attracted attention in the recent years due to the benefits gained by the presence of electrostatic interactions (beyond the hydrophobic) that influence remarkably the association phenomena as well as the rheological behavior [8–15]. Moreover, these associative polymers can be designed to respond to external stimulus like pH [15–17], temperature and ionic strength [18] when weak polyelectrolyte chains are used as the main hydrophilic part of the polymer.

Block copolymer polyampholytes are another interesting class of responsive associative polymers (under a broader definition) bearing oppositely charged blocks which can interact with each other forming hydrophobic sequences, or changing their charge sign from positive to negative upon pH variation. Up to now several well-defined block polyampholytes of various architectures, from simple AB diblocks [19–27] to ABA triblocks [28–30] and ABC [31–40] or A(B-*co*-C) [41] terpolymers as well as star-shaped of A_nB_n [42] and/or $A_n(B–b–C)_n$ [43] topologies have been prepared by "living" polymerization methods. Their study in aqueous solutions showed their ability to self-assemble forming micellar structures, but also three dimensional networks [28–30], through intermolecular electrostatic interactions, exhibiting interesting rheological properties.

In this paper we present a novel class of associative polymers based on a multisegmental ABCBA pentablock terpolymer architecture [44]

* Corresponding author. Department of Chemical Engineering, University of Patras, 26504 Patras, Greece. Tel.: +30 2610 969531; fax: +30 2610 997266.
E-mail address: ct@chemeng.upatras.gr (C. Tsitsilianis).

0032-3861/$ – see front matter © 2008 Elsevier Ltd. All rights reserved.
doi:10.1016/j.polymer.2008.04.058

which constitutes a triblock polyampholyte end-capped at both ends by hydrophobic blocks. The novelty of this associative polymer with respect to the classical ABA non-ionic as well as to the telechelic polyelectrolytes is that the bridging chains of the formed reversible hydrogel can be transformed from positively charged, to negatively charged, by adjusting the pH and/or dielectric constant of the medium. Preliminary results have also shown that in a certain pH range below the isoelectric point, where electrostatic interactions among oppositely charged moieties are present, an intensive thermothickening phenomenon was observed showing that this kind of pentablock terpolymers could be used as multifunctional responsive materials [45].

2. Experimental part

2.1. Synthesis

A poly(methyl methacrylate)–poly(*t*-butyl acrylate)–poly(2-vinyl pyridine)–poly(*t*-butyl acrylate)–poly(methyl methacrylate) (PMMA–P*t*BA–P2VP–P*t*BA–PMMA) pentablock terpolymer precursor was synthesized by "living" anionic polymerization using sodium tetraphenyl diisobutane as a bifunctional organometallic initiator. The reaction was carried out in THF solution, under argon atmosphere at −78 °C during the addition/reaction of 2-vinyl pyridine and at −65 °C for *tert*-butyl acrylate and methyl methacrylate, polymerization. The three monomers were distilled twice under vacuum prior to use in order, to remove protonic impurities. The 2VP monomer was first distilled over sodium wire and then over calcium hydride after being dried overnight, while the last two monomers were first distilled over calcium hydride, and then treated with triethylaluminium solution in hexane. Each monomer was added to the reactor drop wise. During the addition/reaction of 2VP, the solution colorized into dark red and it was followed by the discoloration to pale yellow when the first few drops of the second monomer were added. Finally, the reaction was terminated by the addition of a few drops of methanol. The polymer was precipitated in cold hexane, re-dissolved in benzene, filtered and freeze-dried.

The acid catalyzed hydrolysis of the P*t*BA to PAA blocks was carried out in 1,4-dioxane with 10-fold excess of fuming hydrochloric acid 37% (wt/wt), at 80 °C for 24 h. The degree of hydrolysis was more than 97%.

2.2. Size exclusion chromatography (SEC)

Molecular weight distributions (M_w/M_n) were determined by SEC. The SEC equipment consisted of a Marathon II HPLC pump, Shodex RI-101 refractive index detector and two PLgel MiniMix columns "C" and "D". Calibration was carried out using PS standards. The eluent (THF containing 1% v/v triethylamine in order to prevent adsorption of P2VP blocks in the columns) was delivered at a flow rate of 0.5 mL/min.

2.3. Nuclear magnetic resonance (NMR)

^{1}H NMR spectra were measured on a Bruker AC-400 spectrometer using $CDCl_3$ and d_4-methanol/$CDCl_3$ mixture for precursor (PMMA–P*t*BA–P2VP–P*t*BA–PMMA) and hydrolyzed terpolymer (PMMA–PAA–P2VP–PAA–PMMA), respectively. ^{1}H NMR measurements were used in order to determine the monomer repeating unit composition of the terpolymer, as well as the degree of hydrolysis of the final product.

2.4. Static light scattering

The M_w of the terpolymer was determined by Static light scattering using a thermally regulated (±0.1 °C) spectrogoniometer model SEM RD (Sematech, France) equipped with a He–Ne laser (632.8 nm). The refractive index increment dn/dc, required for the interpretation of the light scattering measurements was determined using the known values of each block and the monomer composition (dn/dc = 0.1). The molecular characteristics of the copolymers under investigation are summarized in Table 1.

2.5. Dynamic light scattering

Auto-correlation functions $g(q,t)$ were measured at a given wave vector, [$q = (4\pi n/\lambda)\sin(\theta/2)$ (n is the refractive index of the solvent)], on a broad time scale with a full multiple digital correlator (ALV-5000/FAST) equipped with 280 channels. The light source was an argon-ion laser (Spectra Physics 2020) operating in single mode at 671 nm with a constant output power of about 220 mW.

The correlation functions were analyzed by the constrained regularized CONTIN method through CoVA-Jacek Gapinski 2001 software. The apparent diffusion coefficients, $D_{app} = \Gamma/q^2$, were determined at the peak of the decay rate distributions and the apparent hydrodynamic radii via the Stokes–Einstein equation

$$R_{h,app} = K_B T/(6\pi\eta D_{app}) \quad (1)$$

where K_B is the Boltzmann constant and η is the viscosity of the solvent at temperature T.

2.6. Electrophoresis

Zeta-potential measurements were carried out at 25 °C, using a Zeta-sizer Nano ZS (Malvern Instruments Ltd.) equipped with a DTS1060C-clear disposable zeta cell (cross-beam mode) and laser light with wavelength 532 nm.

2.7. Rheological measurements

The linear and non-linear rheological properties of the polymeric solutions in methanol/H_2O mixtures, at pH = 8.3 and pH = 2, were studied at 25 °C, using a stress controlled rheometer (Rheometrics Scientific SR200), equipped with a cone-plate geometry (diameter 25 mm, cone angle 5,7°, truncation 56 μm). All steady state viscosities were determined as limits of the transient viscosities following the criterion: time evolution of the transient viscosity lower than 1% during 1 min.

Table 1
Molecular characteristics of the ABCBA pentablock terpolymers

Polymer	M_w/M_n[a]	M_w	P2VP [wt%][c]	PtBA/PAA [wt%][c]	PMMA [wt%][c]
$PMMA_{119}$–$PtBA_{355}$–$P2VP_{296}$–$PtBA_{355}$–$PMMA_{119}$	1.10	146,000[b]	21.3	62.4	16.3
$PMMA_{119}$–PAA_{355}–$P2VP_{296}$–PAA_{355}–$PMMA_{119}$		106,000[d]	29.3	48.2	22.5

Subscripts denote weight average degree of polymerization of each block.
[a] Measured by SEC in THF.
[b] Measured by SLS.
[c] Calculated by ^{1}H NMR.
[d] From the M_w of the pentablock precursor assuming quantitative hydrolysis of the PtBA blocks.

2.8. Atomic force microscopy

Multimode AFM instrument (Digital Instruments, Santa Barbara) was operated in the tapping mode. Silicon tips with radius of 10–20 nm, spring constant of 30 N/m and resonance frequency of 250–300 kHz were used. To prepare the sample, the drop of investigated solution was placed on mica for 30 s and then removed by argon flux. Imaging was performed for dried samples at 40% air humidity.

2.9. Sample preparation

All the solutions were prepared by dissolving first the appropriate amount of terpolymer into MeOH and gentle stirring overnight. In the following, filtered (0.2 μm) distilled water adjusted to a given pH was added drop wise under stirring. Finally, correction of pH was carried out by the addition of aqueous HCl or NaOH 1 N solution. For the light scattering experiments all the solutions were filtered through a 0.45 μm PTFE hydrophilic millipore filter before use. For the concentrated solutions (gels) the dissolution was performed at room temperature (20–25 °C), using vigorous stirring and centrifugation for homogenisation.

3. Results and discussion

3.1. Phase behavior in aqueous media

A well-defined multisegmental pentablock terpolymer of the type $PMMA_{119}$–PAA_{355}–$P2VP_{296}$–PAA_{355}–$PMMA_{119}$ was synthesized by "living" anionic polymerization and characterized through standard analytical methods as described in a recent communication [45]. The solubility of this amphiphilic terpolymer in aqueous media is complex which is due to the monomer composition and the different nature of the constituent building blocks: PMMA is hydrophobic, P2VP is hydrophilic in acidic media and turns hydrophobic at pH > 5 and PAA is marginally soluble in water in its protonated form (low pH) whereas it is highly soluble in basic media. Moreover, in a certain pH range the protonated positively charged P2VP repeating units interact with the negatively charged PAA units (polyampholytic character) complicating further the solubility in water. Therefore the study of the polymer in solution was accomplished in aqueous media in the presence of methanol (MeOH) which is good solvent for P2VP and PAA and bad solvent for PANa (polysodiumacrylate) and PMMA.

The terpolymer under investigation as mentioned above should exhibit the characteristics of polyampholytes since it bears a central P2VP block, which is protonated at low pH behaving as a weak polybase and two PAA blocks that are deprotonated at high pH behaving as weak polyacid. These pH dependent properties were investigated first in a H_2O/MeOH (70/30 v/v) binary solvent mixture.

Electrophoresis measurements were accomplished in a series of solutions of 0.2 wt% polymer concentration of different pH. In Fig. 1 the zeta potential of the solutions has been plotted as a function of pH revealing an isoelectric point, iep (zero charge density) at pH 3.2. Around iep the polymer precipitates as depicted by the digital photos in Fig. 1.

Three pH regions can be distinguished from Fig. 1: the low pH region where homogeneous solutions were obtained, the two-phase (precipitation) region 2.1 < pH < 4.5 and the high pH region where turbid solutions initially are formed (around pH 5) which then turn transparent above pH ~ 6. Evidently the observed precipitation is mainly due to neutralization between the protonated positively charged 2VP moieties and the negatively charged AA units. Moreover, the terpolymer is positively charged in the low pH region while it becomes negatively charged at high pH exhibiting

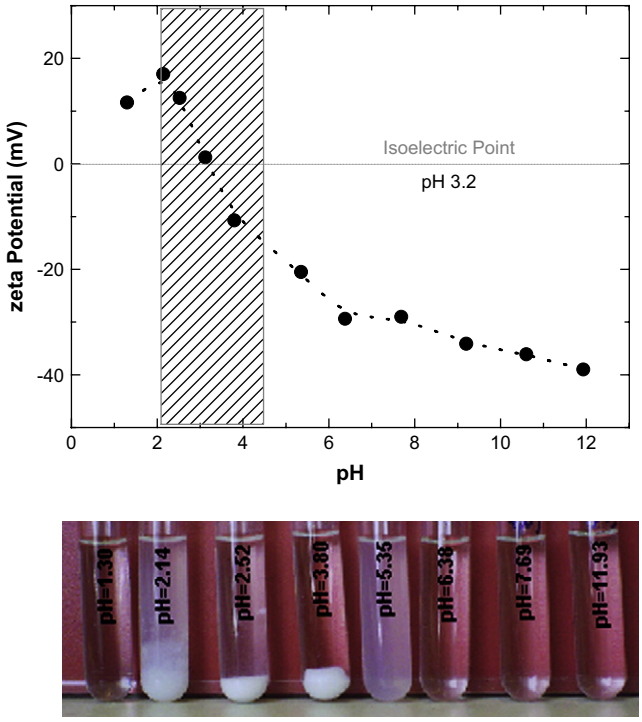

Fig. 1. Zeta-potential of the PMMA–PAA–P2VP–PAA–PMMA pentablock terpolymer at several pH, in a 30:70 MeOH/H_2O mixture and $C_P = 0.2$ wt%. The digital photo shows terpolymer/MeOH/H_2O solutions at different pHs.

therefore in both cases amphiphilic behavior (Scheme 1). The insoluble two-phase region as well as the iep of the particular ampholytic system (P2VP/PAA) depend on the acid to base molar ratio ([AA]/[2VP]) as have been observed for other block copolymers or terpolymers, irrespective of the topology of the polymer segments. For PAA–P2VP–PAA ([AA]/[2VP] = 0.42) iep was determined at pH 5.5 [28] while for P2VP–PMMA–PAA which is similar in nature with the present polymer, iep was shifted to pH 4.5 as the [AA]/[2VP] ratio was increased to 1.22 [39]. The fact that the PMMA–PAA–P2VP–PAA–PMMA exhibits even lower iep at pH 3.2, should be due to even higher acid to base molar ratio ([AA]/[2VP] = 2.4). It should be mentioned here that recently an unexpected shift of iep at pH 2 was observed for the highly asymmetric P2VP–PAA–PnBMA terpolymer ([AA]/[2VP] = 16) [16]. Provided that the pKs of the P2VP and PAA homopolymers are 5 and 5.6, respectively, it seems that the effective pK of PAA segments may be shifted to lower values in the presence of polybase [46].

3.2. Association phenomena in the low pH region

The polymer under investigation in fact is a triblock polyampholyte [28] end-capped by PMMA hydrophobic blocks which

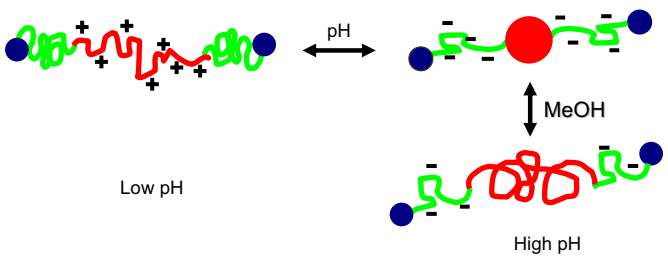

Scheme 1. Shematic representation of the PMMA–PAA–P2VP–PAA–PMMA [PMMA (blue), PAA (green), P2VP (red)] pentablock terpolymer conformation at different conditions of pH and MeOH content. (For interpretation of the references to colour in this scheme legend, the reader is referred to the web version of this article.)

should act as stickers in water. This macromolecular topology suggests that, irrespective of the pH dependent behavior of the central hydrophilic part of the polymer, it will be self-organized at least through hydrophobic interactions in aqueous media. Dynamic light scattering experiments were involved to monitor the association phenomena firstly in the low pH region and in the binary solvent mixture MeOH/H_2O (30:70 v/v).

Characteristic auto-correlation functions along with the distribution of relaxation times, obtained by CONTIN analysis, for several polymer concentrations are demonstrated in Fig. 2. At low concentrations (i.e. $C_p = 0.05$ and 0.1 mg/ml) a rather broad single relaxation mode appeared corresponding to apparent hydrodynamic radius $R_H = 235$ nm as calculated using the Stokes–Einstein equation for spherical particles. This peak should be attributed to the diffusion of micellar clusters of broad distribution as it will be shown by AFM direct observation.

At a higher concentration (i.e. $C_p = 0.5$ mg/ml) the peak observed at lower concentrations has been split to two peaks, while a third peak of very slow relaxation mode has appeared. The corresponding hydrodynamic size of the two first populations (assuming translational diffusion of particles) was determined to be 62 nm and 398 nm. The two faster relaxation modes should be correlated with spherical micelles and micellar clusters, respectively. The slow mode seen at relaxation times of the order of 500–1000 ms (corresponding to apparent hydrodynamic size of 54 μm) should be ascribed to the appearance of the gel phase [12]. Finally at an even higher concentration ($C_p = 1.5$ mg/ml) two well-dissolved relaxation peaks with hydrodynamic sizes of $R_H = 48$ nm and $R_H = 428$ nm were observed that coexist with the gel phase [47]. Similar results have been reported for telechelic polyelectrolytes [12,48]. The dynamic light scattering results demonstrated a rapid growth of micellar clusters towards a three dimensional network. As reported for diblock PAA–PMMA association behavior, for sufficiently long PMMA blocks (ca. 70 units) no detectable polymer exchange occurs on the time scale of weeks which is due to the glassy nature of the PMMA stickers [49]. Therefore the system is not at equilibrium (kinetically frozen) and the size of the various self-assemblies observed by dynamic light scattering depends on preparation history. This also may account for why the plateau of the correlation function is smaller for $C_p = 1.5$ mg/ml than for $C_p = 0.5$ mg/ml. Moreover, CONTIN analysis reports intensity-weighted distributions and the proportion of the large particles is strongly exaggerated, as the scattering intensity is strongly dependent on the radius of the particles ($\sim R^3$ for spherical particles) [50]. Thus, the weight fraction of the larger aggregates is actually rather small.

In order to get information on the morphology and the structural characteristics of the aggregates observed by light scattering, AFM experiments were carried out in the tapping mode. Fig. 3 shows AFM topographies of various self-assemblies deposited on mica substrate from 1 mg/ml solution of pH 1. The images are obtained after adsorption of the molecules/micelles from solution at indicated condition to mica surface and subsequent fast drying of the samples. Similar topographies were obtained also at pH 2. In the magnified image, isolated spherical micelles together with micellar clusters of irregular shape and size can be observed. This direct observation reveals that the elemental self-assembly is likely a flower-like micelle of core–shell–corona internal structure as dictated by the topology and the specific nature of the blocks of the PMMA–PAA–P2VP–PAA–PMMA pentablock terpolymer. The internal hydrophobic core is constituted of the PMMA associated end-blocks of several terpolymers surrounded by the next PAA soluble blocks, located in the internal shell layer, while the external corona is constituted of positively charged protonated P2VP looping chains (Scheme in Fig. 3f). One should, however, keep in mind

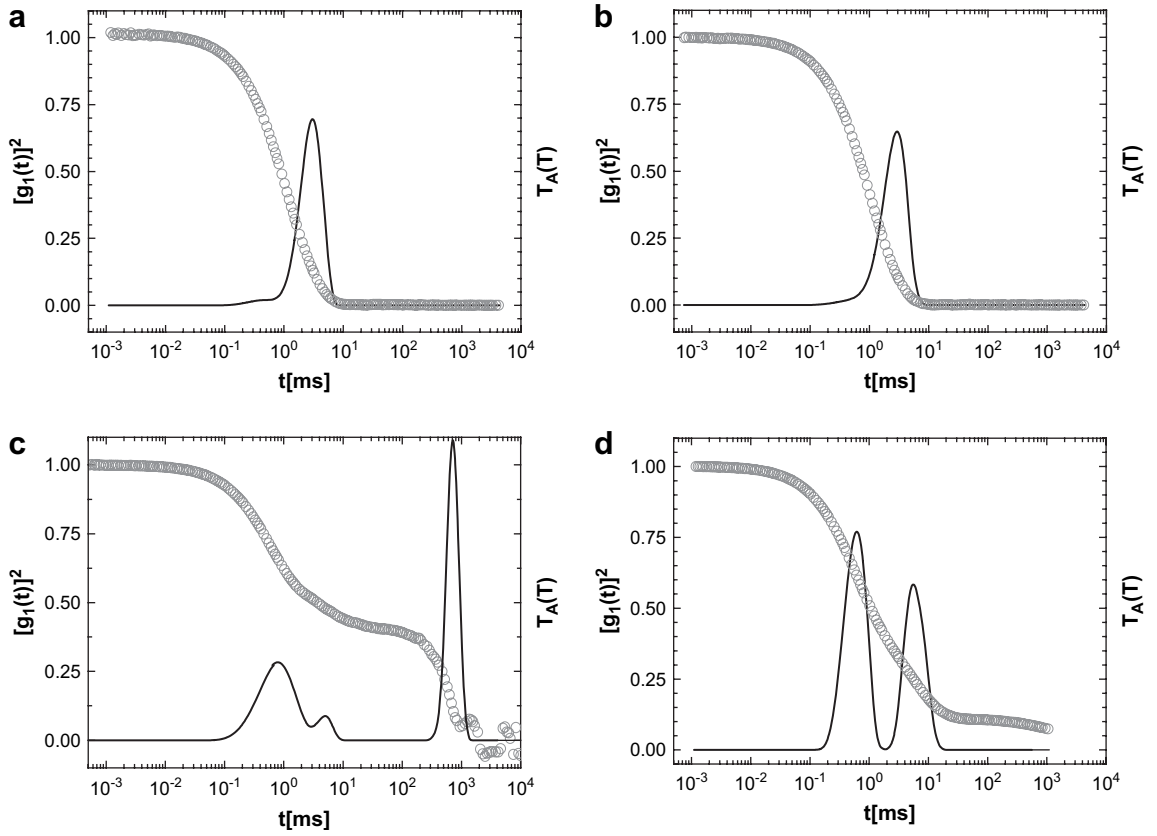

Fig. 2. Correlation function along with the inverse Laplace transformation performed by CONTIN analysis, for concentrations of (a) 0.05 mg/ml; (b) 0.1 mg/ml; (c) 0.5 mg/ml and (d) 1.5 mg/ml PMMA–PAA–P2VP–PAA–PMMA polymeric solution, at pH 2 and scattering angle 90°, in a 30% [v/v] methanol/H_2O mixture.

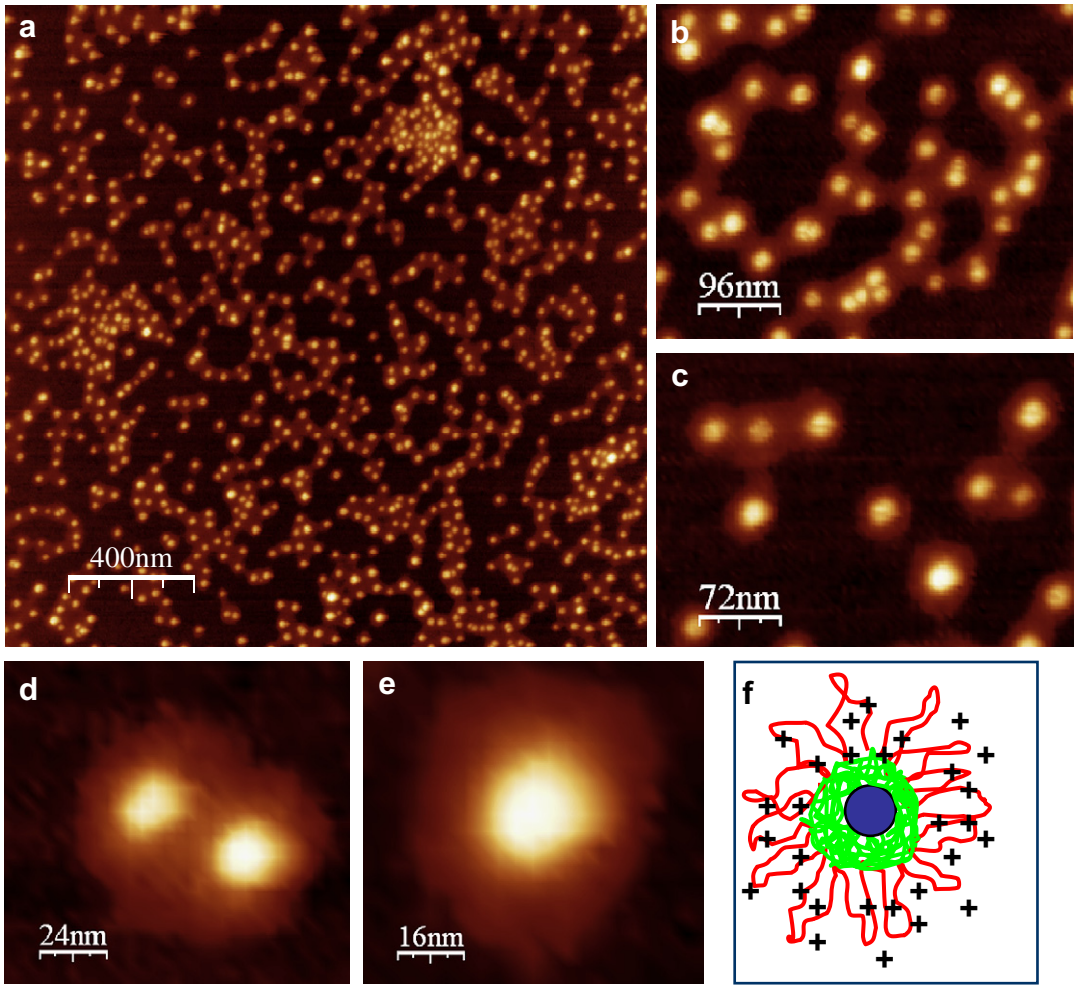

Fig. 3. (a) Atomic force topography of PMMA–PAA–P2VP–PAA–PMMA pentablock terpolymer deposited on mica substrate from 1 mg/ml aqueous solutions at pH 1. Magnifications from (a): (b) micellar strands; (c) associated micelles; (d) twin micelle; (e) single micelle; (f) schematic model of core–shell–corona micellar structure at low pH [PMMA (blue), PAA (green), P2VP (red)]. (For interpretation of the references to colour in this figure legend, the reader is referred to the web version of this article.)

that AFM images are taken in dry state and structures could be influenced by preparation. The correspondence between LS and AFM provides evidence that AFM pictures resemble most significant aspects of structures from solution. Furthermore, in the low pH under investigation the PAA units are almost uncharged and therefore attractive electrostatic interactions with the protonated P2VP units should be considered negligible.

The repulsive interactions between the positive charges along the central P2VP block that form the loops in the corona promote loop to bridge transitions that lead to twin micelles (Fig. 3d) and/or micelle clustering and eventually to a three dimensional transient network upon concentration increase. The above proposed mechanism results in a macroscopic free-standing physical gel as depicted in the inset of Fig. 4.

The steady shear viscosity profile of a 2 wt% polymer solution obtained by a stress controlled rheometer is depicted in Fig. 4 in a viscosity versus shear stress plot. A Newtonian plateau was established at low shear stresses followed by a dramatic decrease of viscosity more than four orders of magnitude revealing a strong shear thinning effect characteristic of the behavior of reversible injectable hydrogels formed by telechelic polyelectrolytes [11,12]. The zero-shear viscosity for $C_p = 2$ wt% was determined at ca. 1300 Pa s to be about six orders of magnitude higher than that of the aqueous medium suggesting strong gelling efficiency of the pentablock associative polymer. The system is also characterized by an apparent yield stress of 5 Pa and elastic modulus, G' (1 Hz), of 25 Pa. In the inset of Fig. 4 the concentration dependence of the zero-shear viscosity, η_0, is also illustrated. The critical gel concentration was roughly estimated at ca. 1.5 wt%.

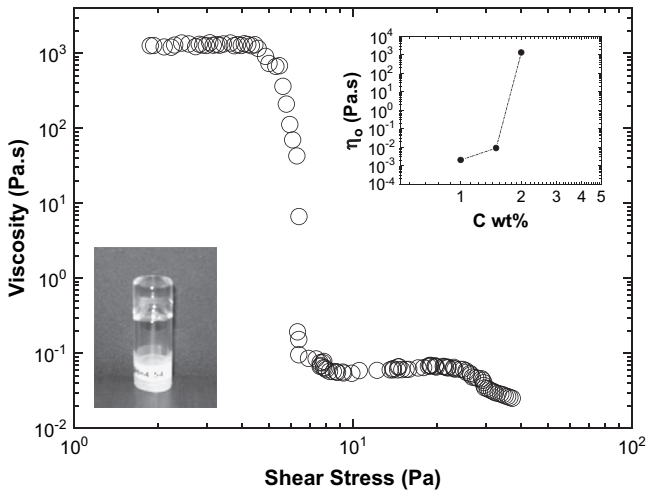

Fig. 4. Shear viscosity as a function of shear stress of PMMA–PAA–P2VP–PAA–PMMA 2 wt% polymer concentration at pH 2.0, in a 30% [v/v] MeOH/H_2O mixture at 25 °C. Insets: digital photo of the formed free-standing gel and double logarithmic plot of the zero-shear viscosity, η_0, as a function of concentration.

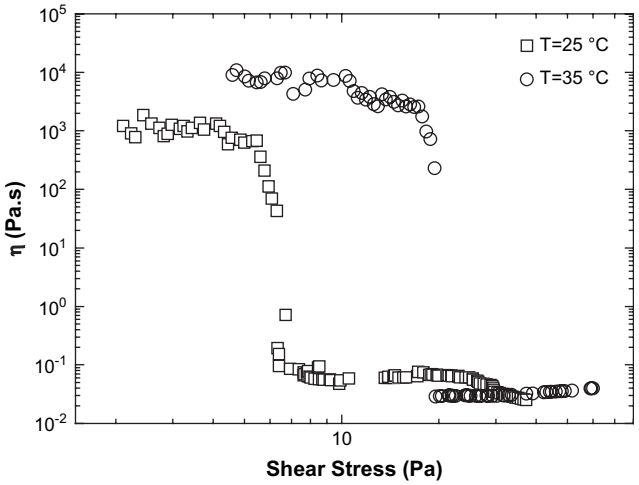

Fig. 5. Shear viscosity as a function of shear stress for a 2 wt% of PMMA–PAA–P2VP–PAA–PMMA, in a 30% [v/v] MeOH/H_2O mixture solution, at pH 2 for 25 °C and 35 °C.

The temperature effect on the gel is also interesting. As shown in Fig. 5 the zero-shear viscosity increases about one order of magnitude upon heating from 25 to 35 °C revealing a thermothickening phenomenon. Moreover, the apparent yield stress increases from 5 to 20 Pa suggesting a substantial strengthening of the network. This effect is likely to be due to the swelling of the PAA segments (including H-bonding breaking) that favors loop to bridge transitions which lead to an increase of the elastically active chains. The fact that the opposite effect was observed for the $PMMA_{43}$–PAA_{24}–$P2VP_{650}$–PAA_{24}–$PMMA_{43}$/water system at the same pH, should be attributed to the very short PAA segments as compared to the present system [45].

3.3. Association phenomena in basic water/methanol solvent mixture

At the high pH region (pH > 5) the nature of the terpolymer is altered substantially since P2VP becomes hydrophobic, increasing therefore the overall hydrophobicity of the polymer. On the other hand the deprotonation of the PAA segments (neutralization by NaOH) increases the hydrophilicity favoring solubility in aqueous media. Moreover, the polymer topological characteristics have been changed since we have three hydrophobic segments interconnected by negatively charged polyelectrolyte chains. In fact the PAA potentially elastic chains between adjacent PMMA hydrophobic domains are interrupted by a hydrophobic P2VP segment which should affect the structure of the network formed at low pH.

In the following we explore the influence of the MeOH content of the association/gelation phenomena keeping the pH constant at 8.3 where the PAA segments are fully charged (100% ionization). Since MeOH is a bad solvent for the PMMA end-blocks the main effect of the solvent selectivity variation is expected to occur on the solubility of the P2VP and PANa segments (potentially elastic chains).

In Fig. 6 the Newtonian viscosity has been plotted as a function of MeOH content for 1 wt%, polymer concentration. As can be observed a maximum in viscosity was attained at 30% MeOH. More importantly a SOL–GEL–SOL transition was revealed in the semi-logarithmic plot. The above effect could be ascribed to the opposite solubility effect of MeOH on the P2VP and PANa segments of the potentially elastic chains. More precisely, as the MeOH content increases the P2VP segments start to swell and dissolve whereas the degree of ionization of the PAA segment decreases due to ion condensation promoted by the decrease of the dielectric constant of the medium.

Dynamic light scattering data obtained from solutions of one order of magnitude lower concentrations from those in rheological experiments at different MeOH/H_2O contents are illustrated in Fig. 7. Multiple relaxation peaks were observed for the 10% (v/v) MeOH solution implying the formation of micelles and micellar aggregates as also was confirmed by AFM (see Fig. 8a). This behavior should be ascribed to the strong hydrophobic contribution of the P2VP central block on polymer association and micelle clustering. As the MeOH content increases the number of relaxation peaks corresponding to the various self-assemblies decreases due to P2VP dissolution and in 50% MeOH only one peak was observed. In this latter case, association is driven mainly by the hydrophobic interactions of the PMMA end-blocks.

Fig. 8 demonstrates characteristic AFM images deposited on mica substrate from different MeOH/H_2O solvent mixtures. In fact they show the early stage of the expected network structures arising at least from the PMMA end-block association of the pentablock terpolymer. The most regular and homogeneous micellar network structure was observed at 30 vol% MeOH which seems to be correlated with the maximum shear viscosity observed in Fig. 6. On the contrary, the structure formed at lower MeOH content, where the association action of P2VP blocks is very strong, the network is heterogeneous since big irregular aggregates can be seen (Fig. 8a). Finally at 50 vol% MeOH only small cores probably of PMMA nature are visible. In this case, the network has not been formed at least at 1 wt% polymer concentration as it is supported by the viscosity data (Fig. 6).

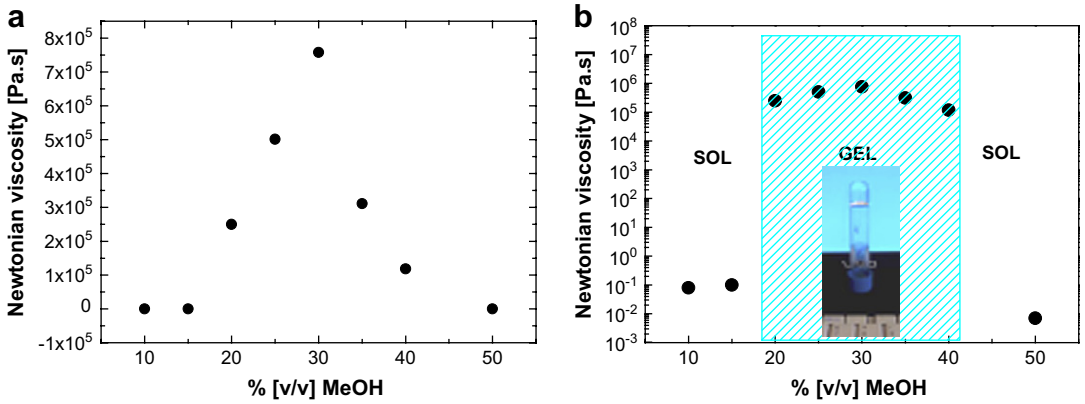

Fig. 6. (a) Newtonian viscosity of 1 wt% polymer solution, in MeOH/H_2O mixtures, as a function of MeOH content, at pH = 8.3, for the PMMA–PAA–P2VP–PAA–PMMA pentablock terpolymer; (b) the same in semi-logarithmic plot showing the SOL–GEL–SOL transition. Inset: digital photo of a free-standing gel of 1 wt% polymer in 30% MeOH/H_2O solvent mixture.

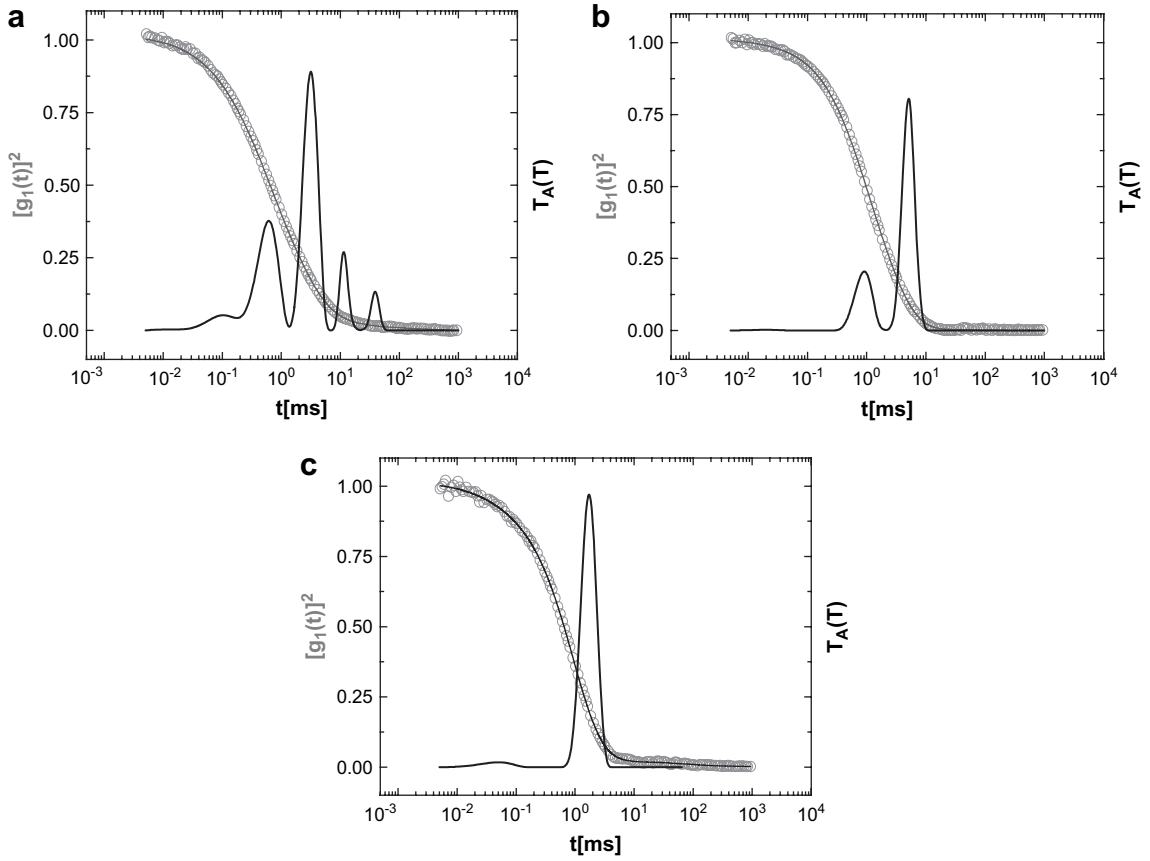

Fig. 7. Correlation function along with the inverse Laplace transformation performed by CONTIN analysis, for a 0.1 wt% PMMA–PAA–P2VP–PAA–PMMA polymeric solution, at pH 8.3 and scattering angle 90°, in (a) 10; (b) 30 and (c) 50% [v/v] MeOH/H_2O mixtures.

The elemental constituents of these networks formed at lower hierarchical level are micellar self-assemblies, the morphology of which depends on the MeOH content of the solution at pH 8.3. At low MeOH content, a possible micellar structure dictated also from the PMMA–PAA–P2VP–PAA–PMMA topology and preparation process (initial dissolution in MeOH) could be multicompartment micelles [51] comprising a PMMA central core surrounded by several P2VP cores of smaller size (Scheme in Fig. 9a) as it is suggested from the AFM image in Fig. 9a.

This morphology is driven from two antagonistic interactions: the attractive hydrophobic interactions among the PMMA and P2VP cores and the repulsive electrostatic interactions along the PAA interconnecting segments. The latter seems to predominate, preventing collapse of the P2VP domains on the PMMA central core.

At 30 wt% MeOH, due to lowering of the dielectric constant of the medium, which provokes ion condensation of the counter ions that weaken the repulsive short range interactions along the PAA blocks, the attractions of the different hydrophobic domains seems to predominate, leading to micelles constituted of a centrosymmetric core and PAA negatively charged corona (Fig. 9b). The incompatibility factor, expressed by the product of $\chi_{AC}N$, where χ_{AC} is the interaction parameter and N is the number of the repeating units ($N_A + N_C$), was calculated to be 59, which suggests segregation of the different hydrophobic domains and the formation of a compartmentalized core [52]. AFM cannot provide details of the core internal structure, i.e. the nature of internal core may be either PMMA or P2VP. However, in the conditions of 30% MeOH, PMMA block-ends should be associated first, located then in the core interior (Scheme in Fig. 9b).

By further increasing the MeOH content, the core size is decreasing, implying that part of the P2VP intermediate core layer starts to swell and is dissolved in the medium as observed by AFM (Fig. 10). At 50% MeOH, only small cores are visible in AFM images which are very likely to be formed only by PMMA block association. In this case flower-like micelles should be formed with PAA–P2VP–PAA looping chains. Since the micelles still exhibit negative zeta potential, repulsive interactions along the corona chains still exist which may also push out the P2VP swollen segments in the periphery of the micellar corona (Scheme in Fig. 9c). Moreover, the zeta-potential levels off at 50% MeOH (Fig. 11) implying that further diminishing of the dielectric constant does not affect the charge density on the particle surface [53].

The observed decrease of the repulsions along the potentially bridging chains (arisen from ion condensation) with respect to those at lower MeOH content, seems to prevent loop to bridge transitions inducing a GEL–SOL transition as observed by a dramatic drop of the viscosity (Fig. 6). In these conditions higher polymer concentration is needed to build the 3D network.

In the following, we focus on the rheological properties of the physical gel at the conditions of pH 8.3 and 30% MeOH, where the viscosity maximum was observed. The growth of the network was monitored by measuring the zero-shear viscosity as a function of concentration in a stress controlled rheometer. The concentration dependence of the zero-shear viscosity, η_0, is presented in Fig. 12, from which the critical gel concentration was determined to be 0.77 wt%. At concentration of about 1 wt%, the viscosity raises about eight orders of magnitude with respect to that of the medium revealing a very intensive thickening behavior.

Oscillatory shear measurements were conducted first to establish the linear viscoelastic regime. As can be observed in Fig. 13a the network collapses at relatively high deformation of about 10% shear strain, differing significantly from the fragile behavior (linear

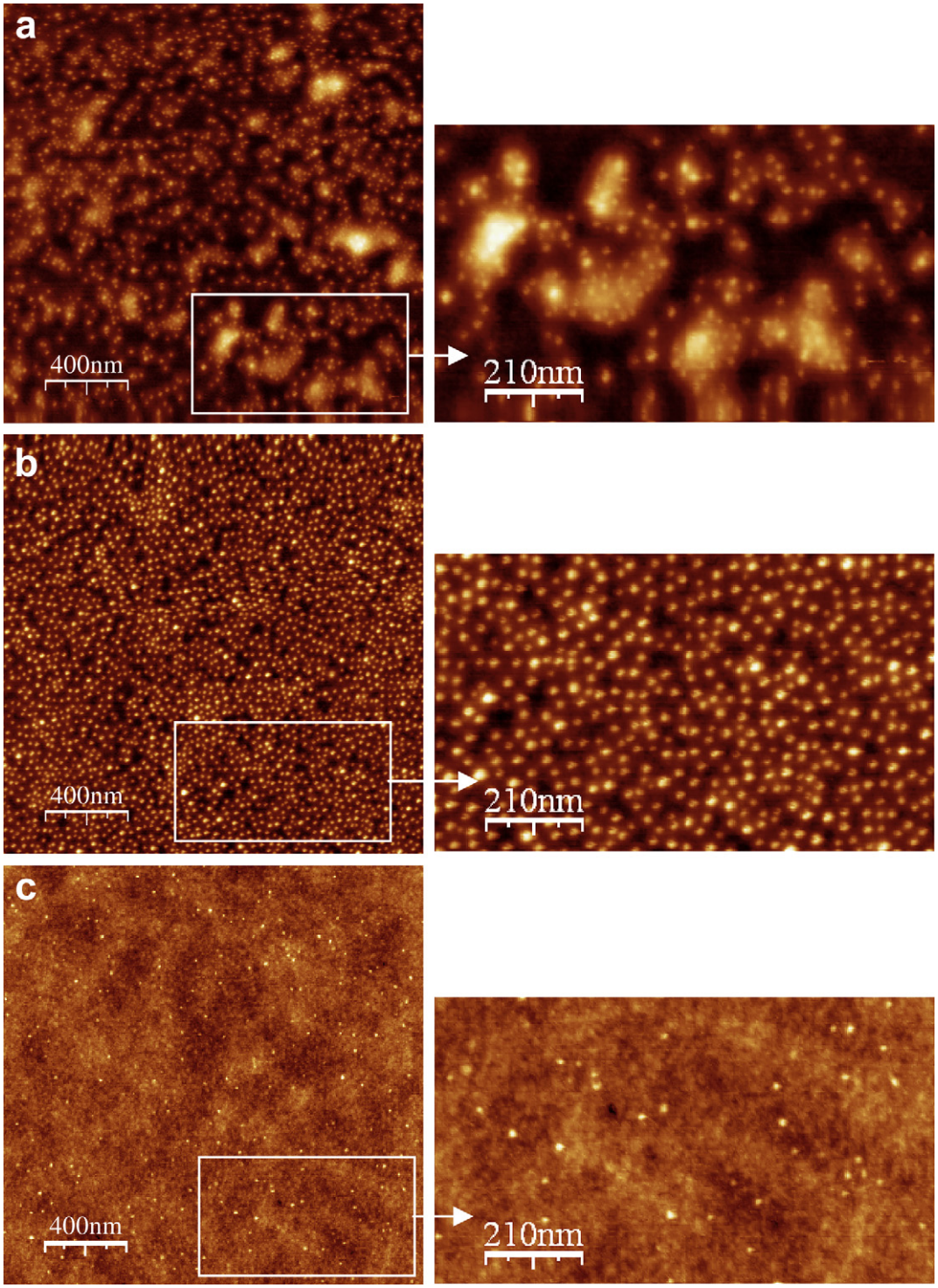

Fig. 8. Atomic force microscopy topography of PMMA–PAA–P2VP–PAA–PMMA pentablock terpolymer from different MeOH/H_2O (pH 8.3) mixtures and $C_p = 2$ mg/ml in: (a) 20/80; (b) 30/70 and (c) 50/50% [v/v].

viscoelastic limit at about 1% shear strain) of the telechelic polyelectrolytes in which the elastic chains are constituted only by stretched (charged) PAA chains [10]. This behavior should be ascribed to the central swollen P2VP "spacer" of the PANa–P2VP–PANa elastic chains that may absorb the applied stress and the less stretched conformation of PAA, due to the lower dielectric constant of the medium (presence of MeOH). Frequency sweep experiment was then performed in the linear viscoelastic regime, where the network structure remains intact.

These measurements have shown that at 1 wt% polymer concentration, the system behaves already as a strong physical gel, since the storage modulus, G', is about one order of magnitude greater than the loss modulus, G'' (Fig. 13) and the G'–G'' intersection is not visible as it has been shifted to very low frequencies. The latter implies that the characteristic time, t_c, of the fluid is longer than 500 s (lowest measured frequency) which is consistent with the characteristics of an elastic soft material.

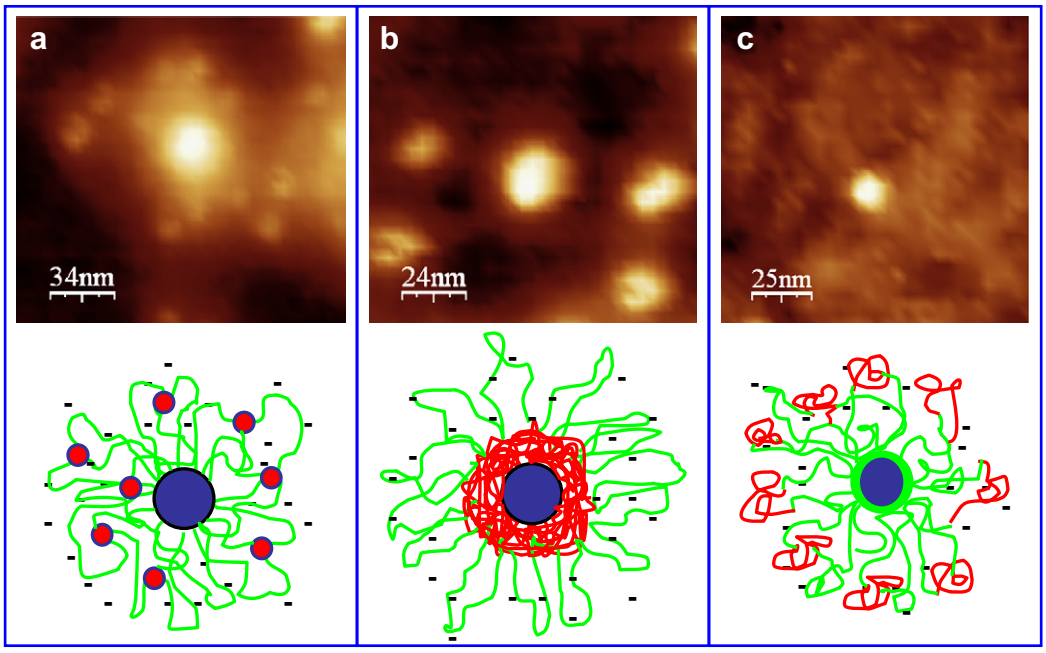

Fig. 9. Atomic force microscopy images and schematic representation of micellar self-assemblies of the terpolymer [PMMA (blue), PAA (green), P2VP (red)] at pH = 8.3 from different MeOH/H_2O mixtures in: (a) 20/80; (b) 30/70 and (c) 50/50% [v/v]. (For interpretation of the references to colour in this figure legend, the reader is referred to the web version of this article.)

Interesting information was also obtained by increasing/decreasing stress sweep tests illustrated in Fig. 14. A very pronounced hysteresis phenomenon was observed again substantially different from those observed in telechelic polyelectrolytes [10] and triblock polyampholytes [29].

A smooth shear thickening effect was first observed followed by an extended Newtonian plateau and a dramatic drop of the viscosity when the shear stress exceeds about 100 Pa which implies network deformation (non-linear regime). The recovery of the network structure seems to occur in three steps separated by two

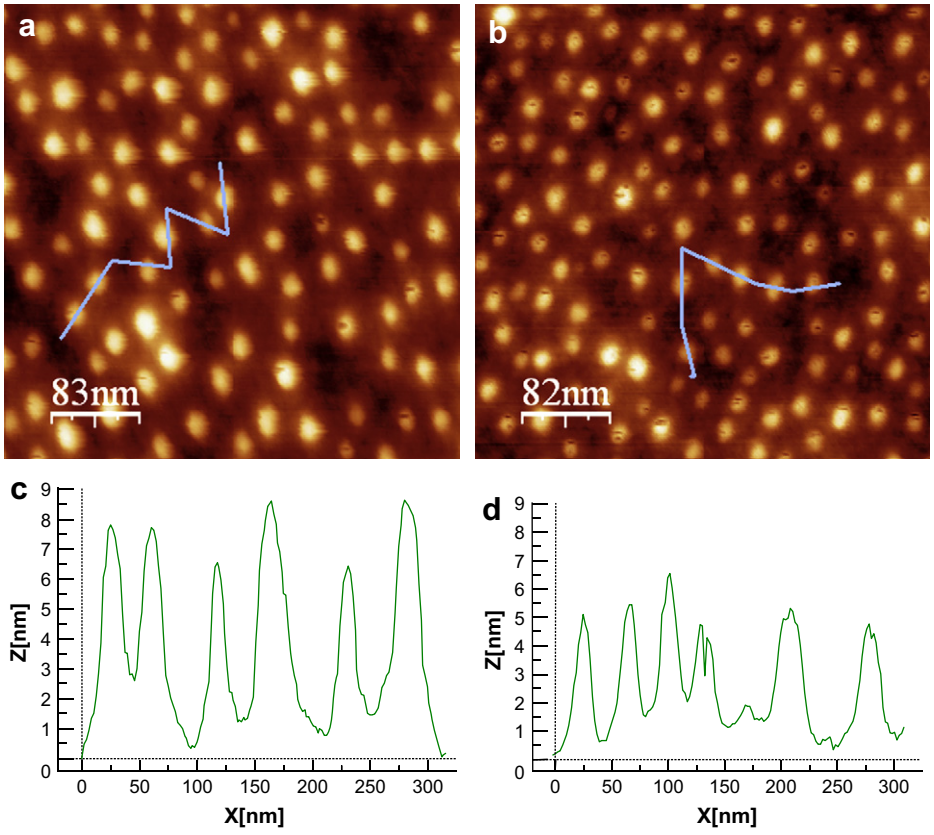

Fig. 10. Atomic force microscopy topographies and height profiles along the lines on micellar network of the terpolymer at pH 8.3 from different MeOH/H_2O mixtures in % [v/v]: (a,c) 30/70 and (b,d) 40/60.

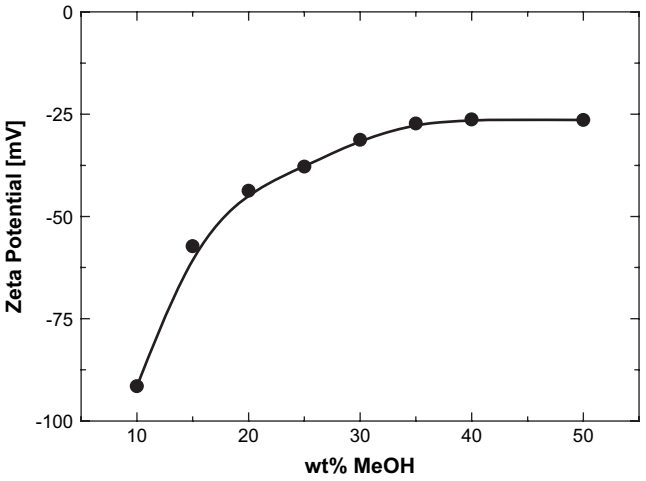

Fig. 11. Zeta-potential as a function of MeOH content of the PMMA–PAA–P2VP–PAA–PMMA pentablock terpolymer ($C_P = 0.2$ wt%) at pH 8.3, in MeOH/H_2O solvent mixture.

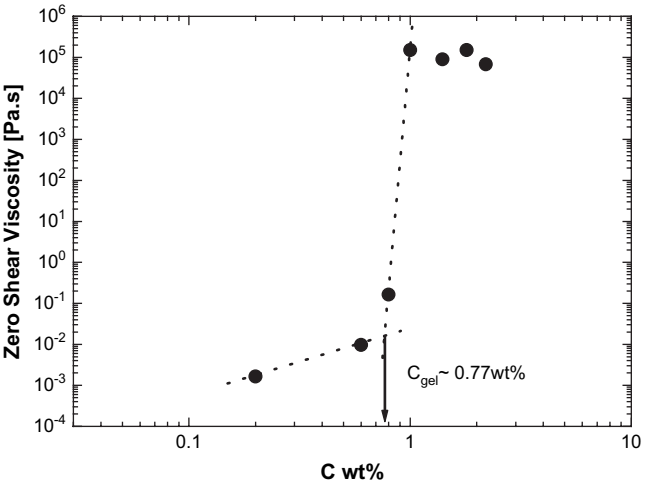

Fig. 12. Double logarithmic plot of the zero-shear viscosity, η_0, as a function of concentration, at pH 8.3, in a 30% [v/v] MeOH/H_2O mixture for PMMA–PAA–P2VP–PAA–PMMA pentablock terpolymer at 25 °C.

abrupt viscosity augmentations upon stress decreasing. Finally it was attained at very low stress, as the viscosity rises up again to 10^5 Pa s, exhibiting therefore pronounced thixotropy. It should be noted that this behavior is characteristic of the high pH gel phase irrespective of the MeOH content.

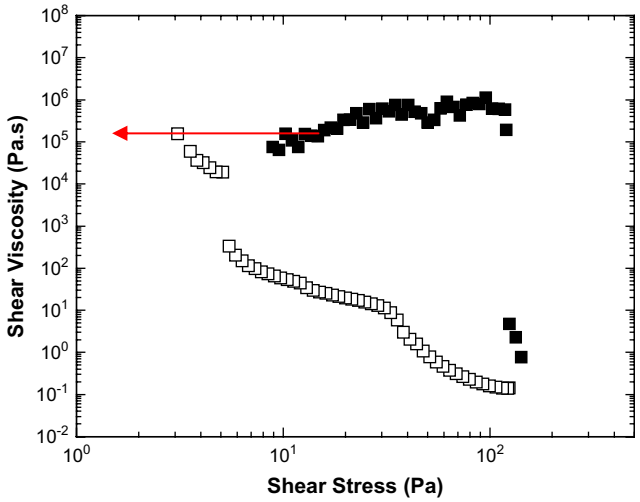

Fig. 14. Circle of increasing (solid symbol)/decreasing (open symbol) shear viscosity as a function of shear stress for a 1 wt% of PMMA–PAA–P2VP–PAA–PMMA, in a 30% [v/v] MeOH/H_2O solvent mixture, at pH 8.3 and 25 °C.

4. Conclusions

A novel associative polymer based on $PMMA_{119}$–PAA_{355}–$P2VP_{296}$–PAA_{355}–$PMMA_{119}$ pentablock terpolymer architecture was designed and explored in aqueous media in the presence of MeOH. Due to the fact that the hydrophilic central part of the terpolymer is constituted of the PAA–P2VP–PAA triblock polyampholyte, which is strongly responsive to pH, this polymer exhibits rich association and gelation phenomena.

By tuning the pH and/or the solvent selectivity and dielectric constant of the medium, we found conditions for the formation of transient networks (hydrogels) of different nature. At low pH the hydrogel is based on a three dimensional network comprising PMMA hydrophobic cores (physical crosslinks) interconnected by complex bridging (elastically active) chains constituted of positively charged P2VP and non-ionic PAA segments. The hydrogel is also temperature sensitive (thermothickening behavior) due to the presence of PAA segments in the elastic chains. At high pH the hydrogel is transformed reversibly to a negatively charged network, the bridging chains of which comprise ionized PAA segments interrupted by a hydrophobic P2VP block, swellable on MeOH addition.

The rheological properties of the hydrogels formed at different conditions exhibit remarkable differences: the high pH gel exhibits significant lower C_{gel} (0.7 wt% versus 1.5%), much higher elastic

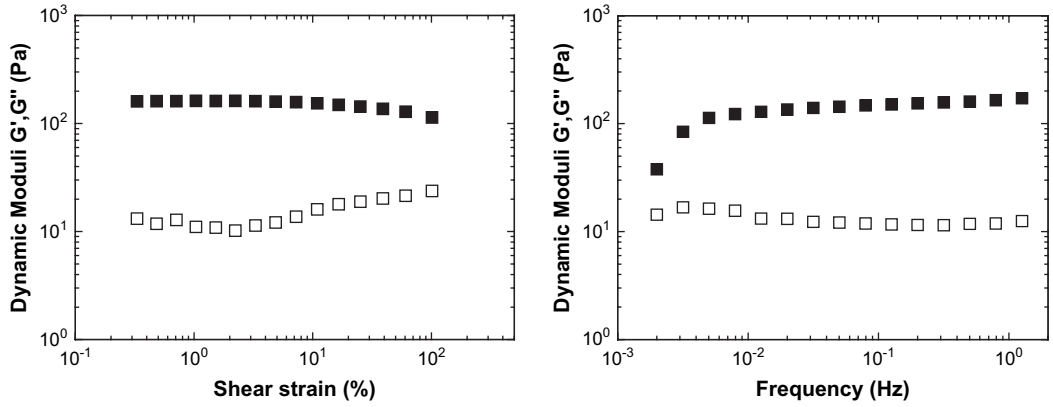

Fig. 13. Dynamic moduli G', G'' as a function of shear strain at 1 Hz frequency (a), and frequency at 1% strain (b), at pH 8.3, in 30% [v/v] MeOH/H_2O mixtures of a 1 wt% PMMA–PAA–P2VP–PAA–PMMA polymer solution, at 25 °C.

modulus G' (1 Hz) (175 Pa versus 25 Pa), apparent yield stress (200 Pa versus 5 Pa) and shear viscosity (two orders of magnitude higher) regarding those of low pH gel. These differences should be ascribed to the nature of the network elastic chains and mainly to the considerably longer length (arisen from electrostatic stretching) in high pH (PAA_{355}–P2VP–PAA_{355}) with respect to that in low pH (PAA–$P2VP_{296}$–PAA). It should be mentioned here that in both type of gels the observed critical gel concentration is significantly lower than those of other non-ionic ABCBA associative polymers reported recently [54–57].

It was also demonstrated that in the high pH regime and 1 wt% polymer concentration, a SOL–GEL–SOL transition occurred, which was induced by varying the MeOH content (affecting solvent selectivity and medium dielectric constant) in the MeOH/H_2O binary solvent mixture. This phenomenon was attributed to the opposite effect of MeOH on the conformation of the different segments of the network elastic chains, i.e. P2VP swelling and PAA unstretching, and the interplay of the hydrophobic and electrostatic interactions.

In all cases micellar type reversible networks formed are constituted of interconnected flower-like micelles that exhibit different features depending on pH and MeOH content. We found conditions for the formation of core–shell–corona micelles with positively charged corona (pH < 2), multicompartment micelles comprising P2VP and PMMA hydrophobic domains (pH 8.3, low MeOH content), micelles constituted of a centrosymmetric compartmentalized core and PAA negatively charged corona (pH 8.3, 30%, 40% MeOH), and core–shell micelles of PMMA core (pH 8.3, 50% MeOH).

To the best of our knowledge the present associative system exhibits a unique very rich behavior responding to various external conditions like pH, temperature, dielectric constant and could constitute a paradigm for further design and development of novel associative polymers towards potential applications in biomedicine, i.e. injectable hydrogels and drug delivery systems.

Acknowledgement

We thank the European Social Fund (ESF), Operational Program for Educational and Vocational Training II (EPEAEK II), and particularly the Program PYTHAGORAS II, for funding the above work.

References

[1] Annable T, Buscall R, Ettelaier R, Whittlestone D. J Rheol 1993;37:695.
[2] Alami E, Almgren M, Brown W, Francois J. Macromolecules 1996;29:2229.
[3] Chassenieux C, Nicolai T, Durand D. Macromolecules 1997;30:4952.
[4] Winnik MA, Yekta A. Curr Opin Colloid Interface Sci 1997;2:424.
[5] Rubinstein M, Dobrynin AV. Curr Opin Colloid Interface Sci 1999;4:83.
[6] Berret J-F, Calvet D, Collet A, Viguier M. Curr Opin Colloid Interface Sci 2003;8:296.
[7] Wang Y, Winnik MA. Langmuir 1990;6:1437.
[8] Tsitsilianis C, Iliopoulos I, Ducouret G. Macromolecules 2000;33:2936.
[9] Tsitsilianis C, Katsambas I, Sfika V. Macromolecules 2000;33:9054.
[10] Tsitsilianis C, Iliopoulos I. Macromolecules 2002;35:3662.
[11] Katsampas I, Tsitsilianis C. Macromolecules 2005;38:1307.
[12] Stavrouli ND, Tsitsilianis C, Kiriy A, Gorodyska G, Stamm M. J Nanostruct Polym Nanocomp 2005;1:15.
[13] Gotzamanis GT, Tsitsilianis C, Hadjiyannakou SC, Patrickios GS, Lupitskyy R, Minko S. Macromolecules 2006;39:678.
[14] Kimerling AS, Rochefort WE, Bhatia SR. Ind Eng Chem Res 2006;45:6885.
[15] Howse JK, Topham P, Crook CJ, Gleeson AJ, Bras W, Jones RAL, et al. Nano Lett 2006;6:73.
[16] Katsampas I, Roiter Y, Minko S, Tsitsilianis C. Macromol Rapid Commun 2005;26:1371.
[17] Bossard F, Aubry T, Gotzamanis GT, Tsitsilianis C. Soft Matter 2006;2:510.
[18] Angelopoulos S, Tsitsilianis C. Macromol Chem Phys 2006;207:2188.
[19] Kamachi M, Kurihara M, Stille JK. Macromolecules 1972;5:161.
[20] Varoqui R, Tran Q, Pefferkorn E. Macromolecules 1979;12:831.
[21] Creutz S, Teyssié P, Jérôme R. Macromolecules 1997;30:6.
[22] Lowe AB, Billingham NC, Armes SP. Chem Commun 1997:1035.
[23] Lowe AB, Billingham NC, Armes SP. Macromolecules 1998;31:5991.
[24] Creutz S, van Stam J, De Schryver FC, Jérôme R. Macromolecules 1998;31:681.
[25] Goloub T, de Keizer A, Cohen Stuart MA. Macromolecules 1999;32:8441.
[26] Liu S, Armes SP. Angew Chem Int Ed 2002;41:1413.
[27] Hadjikallis G, Hadjiyannakou SC, Vamvakaki M, Patrickios CS. Polymer 2002;43:7269.
[28] Sfika V, Tsitsilianis C. Macromolecules 2003;36:4983.
[29] Bossard F, Sfika V, Tsitsilianis C. Macromolecules 2004;37:3899.
[30] Bossard F, Tsitsilianis C, Yannopoulos SN, Petekidis G, Sfika V. Macromolecules 2005;38:2883.
[31] Patrickios CS, Hertler WR, Abbott NL, Hatton TA. Macromolecules 1994;27:930.
[32] Patrickios CS, Hertler WR, Hatton TA. Biotechnol Bioeng 1994;44:1031.
[33] Chen W-Y, Alexandridis P, Su C-K, Patrickios CS, Hertler WR, Hatton TA. Macromolecules 1995;28:8604.
[34] Patrickios CS, Strittmatter JA, Hertler WR, Hatton TA. J Colloid Interface Sci 1996;182:326.
[35] Patrickios CS, Lowe AB, Armes SP, Billingham Nc. J Polym Sci Part A Polym Chem 1998;36:617.
[36] Patrickios CS, Sharma LR, Armes SP, Billingham NC. Langmuir 1999;15:1613.
[37] Giebeler E, Stadler R. Macromol Chem Phys 1997;198:3815.
[38] Bieringer R, Abetz V, Müller AHE. Eur Phys J E 2001;5:5.
[39] Sfika V, Tsitsilianis C, Kiriy A, Gorodyska G, Stamm M. Macromolecules 2004;37:9551.
[40] Tsitsilianis C, Roiter Y, Katsampas I, Minko S. Macromolecules 2008;41:925.
[41] Gotzamanis GT, Tsitsilianis C. Macromol Rapid Commun 2006;27:1757.
[42] Georgiou TK, Phylactou LA, Patrickios CS. Biomacromolecules 2006;7:3505.
[43] Tsitsilianis C, Katsampas I, Roiter Y, Minko S, Stavrouli N, Gotsopoulos M. Polym Preprint 2006;47(2):798.
[44] Tsitsilianis C. Multisegmentals block/graft copolymers. In: Matyjaszewski K, Gnanou Y, Leibler L, editors. Macromolecular engineering: precise synthesis, materials properties, applications, vol. 2. Wiley-VCH; 2007 [chapter 4].
[45] Stavrouli ND, Katsampas I, Angelopoulos S, Tsitsilianis C. Macromol Rapid Commun 2008;29:130.
[46] Mafé S, Garcia-Morales V, Ramirez P. Chem Phys 2004;296:29.
[47] Okabe S, Sugihara S, Aoshima S, Shibayama M. Macromolecules 2003;36:4099.
[48] Schilli CM, Zhang MF, Rizzardo E, Thang SH, Chong YK, Edwards K, et al. Macromolecules 2004;37:7861.
[49] Rager T, Meyer WH, Wegner G, Winnik MA. Macromolecules 1997;30:4911.
[50] Zaroslov Y, Fytas G, Pitsikalis M, Hadjichristidis N, Philippova O, Khokllov A. Macromol Chem Phys 2005;206:173.
[51] Lutz J-F, Laschewsky A. Macromol Chem Phys 2005;206:813.
[52] The Flory interaction parameter χ_{AC} among the P2VP and PMMA segments were calculated as in Ref. [40] using solubility parameter for P2VP and PMMA, 10.0 and 9.08 $(cal/cm^3)^{1/2}$, respectively, estimated from the Hoy method.
[53] Liu F, Eisenberg A. J Am Chem Soc 2003;125:15059.
[54] Shim WS, Yoo JS, Bae YH, Lee DS. Biomacromolecules 2005;6:2930.
[55] Determan MD, Guo L, Thiyagarajan P, Mallapragada SK. Langmuir 2006;22:1469.
[56] Park SY, Lee Y, Bae KH, Ahn C-H, Park TG. Macromol Rapid Commun 2007;28:1172.
[57] He Y, Lodge TP. Macromolecules 2008;41:167.